

Synthesis, X-ray Crystallography, and Computational Analysis of 1-Azafenestranes

Scott E. Denmark,* Justin I. Montgomery, and Laurenz A. Kramps

Contribution from the Roger Adams Laboratory, Department of Chemistry, University of Illinois, Urbana, Illinois 61801

Received May 10, 2006; E-mail: denmark@scs.uiuc.edu

Abstract: The tandem [4+2]/[3+2] cycloaddition of nitroalkenes has been employed in the synthesis of 1-azafenestranes, molecules of theoretical interest because of planarizing distortion of their central carbon atoms. The synthesis of *c,c,c,c*-[5.5.5.5]-1-azafenestrane was completed in good yield from a substituted nitrocyclopentene, and its borane adduct was analyzed through X-ray crystallography, which showed a moderate distortion from ideal tetrahedral geometry. The syntheses of two members of the [4.5.5.5] family of 1-azafenestranes are also reported, including one with a trans fusion at a bicyclic ring junction which brings about considerable planarization of one of the central angles (16.8° deviation from tetrahedral geometry). While investigating the [4.5.5.5]-1-azafenestranes, a novel dyotropic rearrangement that converts nitroso acetals into tetracyclic amins was discovered. Through conformational analysis, a means to prevent this molecular reorganization was formulated and realized experimentally with the use of a bulky vinyl ether in the key [4+2] cycloaddition reaction. Finally, DFT calculations on relative strain energy for the 1-azafenestranes, as well as their predicted central angles, are disclosed.

Introduction

The latter half of the 19th century was an era rife with development for the structural theory of organic chemistry, culminating in the groundbreaking proposal by van't Hoff¹ and LeBel² that the four substituents around a tetracoordinate carbon atom should be positioned at the vertices of a regular tetrahedron. Although controversial at first, the proposal soon gained acceptance, and it is now one of the most powerful scientific theories. However, almost immediately after the publication of the theory, chemists began to probe its limits through the synthesis of molecules that deviate from idealized tetrahedral geometry. In 1884, William Henry Perkin, Jr., published the first syntheses of compounds containing cyclopropane and cyclobutane rings.³ Molecules containing small rings illustrate the most common type of distortion to tetrahedral carbon, the scissor-type distortion, in which one angle around a tetracoordinate carbon atom contracts from the normal bond angle of 109.5° while the opposite angle enlarges. Another type of distortion to tetrahedral carbon, umbrella-type, is best illustrated by cubane systems,⁴ where three of the substituents around a tetracoordinate carbon atom are in close proximity, resulting in considerable angle strain.

A less obvious deformity to tetrahedral carbon results when two opposite angles extend. This flattening of tetracoordinate carbon is known as planarization, and a number of strategies exist to engender this distortion.⁵ The best-studied of these strategies is represented by an interesting family of compounds

called fenestranes^{6,7} that contain a central quaternary carbon atom which serves as a common vertex for four fused carbocycles (Figure 1, **1**). An [*m.n.o.p*]fenestrane has four rings with sizes *m*, *n*, *o*, and *p*. A modified version of the nomenclature introduced by Keese^{7a} that describes the structure and stereochemistry of fenestranes will be used throughout this article. To illustrate, [5.5.5.5]fenestrane **2** is made up of four cis-fused [3.3.0] bicyclic systems (*m*-*n*, *n*-*o*, *o*-*p*, and *p*-*m* bicyclic systems) and is therefore designated a *c,c,c,c*-fenestrane; however, embedded within the ring system of fenestrane **3** is a trans-fused, [3.3.0]-bicyclooctane unit (highlighted in blue, trans-fusion highlighted in red). Therefore, compound **3** is named *c,t,c,c*-[4.5.5.5]-fenestrane. Calculations⁸ have predicted that as ring size is decreased and trans relationships are incorporated, the planarization of the central carbon of a fenestrane will increase.

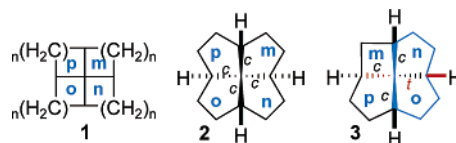


Figure 1. Nomenclature for fenestranes.

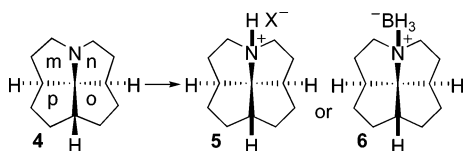
The experimental determination of the extent of planarization at the central carbon of a given fenestrane is best accomplished through X-ray crystallographic analysis. Although a number of X-ray crystal structures of substituted fenestranes have appeared

(1) van't Hoff, J. H. *Arch. Neert. Sci. Exactes Nat.* **1874**, *9*, 445.
 (2) LeBel, J. A. *Bull. Soc. Chim. Fr.* **1874**, *22*, 337.
 (3) Perkin, W., Jr. *Ber. Dtsch. Chem. Ges.* **1884**, *17*, 323.
 (4) Eaton, P. E. *Angew. Chem., Int. Ed. Engl.* **1992**, *31*, 1421–1436.
 (5) Minkin, V. I.; Minyaev, R. M.; Hoffmann, R. *Russ. Chem. Rev.* **2002**, *71*, 869–892.

(6) Venepalli, B. R.; Agosta, W. C. *Chem. Rev.* **1987**, *87*, 399–410.
 (7) (a) Thommen, M.; Keese, R. *Synlett* **1997**, 231–240. (b) Kuck, D. In *Advances in Theoretically Interesting Molecules*; Thummel, R. P., Ed.; JAI Press: Greenwich, CT, 1998; Vol. 4, pp 81–155.
 (8) Hirschi, D.; Luef, W.; Gerber, P.; Keese, R. *Helv. Chim. Acta* **1992**, *75*, 1897–1908.

in the literature,^{8,9} unsubstituted fenestranes are low-molecular-weight hydrocarbons, and they are not crystalline solids at room temperature; therefore, no X-ray crystal structures for these compounds have been reported. By substituting a nitrogen atom for one of the external bridgehead carbons of a fenestrane, opportunities for X-ray analysis of an unsubstituted azafenestrane exist. For example, *c,c,c,c*-[5.5.5.5]-1-azafenestrane **4** (Scheme 1)¹⁰ could be derivatized through salt (**5**) or adduct (**6**) formation to give a crystalline solid that is amenable to solid-state analysis. In addition, through synthesis of a series of azafenestranes with varying ring sizes and stereochemical relationships, the factors that lead to increased planarization could be confirmed experimentally in a system where no carbon ring substituents are present.

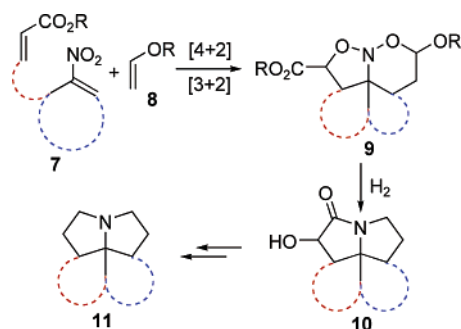
Scheme 1



Because azafenestrane **4** is simply a pyrrolizidine fused to a bicyclo[3.3.0]octane ring system, we planned to apply the tandem [4+2]/[3+2] nitroalkene cycloaddition strategy to the synthesis of **4** and other more strained variants (Scheme 2). A number of pyrrolizidine-based alkaloids have been synthesized in these laboratories utilizing the tandem cycloaddition of nitroalkenes.¹¹ To construct the azafenestrane ring system, cyclic nitroalkenes with tethered dipolarophiles **7** would be required. Intermolecular [4+2] cycloaddition with a vinyl ether **8**, followed by intramolecular [3+2] cycloaddition, would provide tetracyclic nitroso acetals of type **9** which could be converted to the corresponding pyrrolizidinones **10** through hydrogenolysis. Further synthetic manipulation would complete the unsubstituted azafenestranes **11**. This report describes the synthesis of a number of strained 1-azafenestranes, their analysis through X-ray crystallography, and calculations on relative strain energy for this family of compounds.¹²

- (9) (a) Han, W. C.; Takahashi, K.; Cook, J. M.; Weiss, U.; Silverton, J. V. *J. Am. Chem. Soc.* **1982**, *104*, 318–321. (b) Guidetti-Grept, R.; Herzog, B.; Debrunner, B.; Siljegovic, V.; Keese, R.; Frey, H.-M.; Hauser, A.; König, O.; Luthi, S.; Birrer, J.; Nyffeler, D.; Fortsch, M.; Burgi, H.-B. *Acta Crystallogr., Sect. C* **1995**, *51*, 495–497. (c) Thommen, M.; Keese, R.; Fortsch, M. *Acta Crystallogr., Sect. C* **1996**, *52*, 2051–2053. (d) Rao, V. B.; George, C. F.; Wolff, S.; Agosta, W. C. *J. Am. Chem. Soc.* **1985**, *107*, 5732–5739. (e) Wolff, S.; Venepalli, B. R.; George, C. F.; Agosta, W. C. *J. Am. Chem. Soc.* **1988**, *110*, 6785–6790. (f) Smit, W. A.; Buhanjuk, S. M.; Simonyan, S. O.; Shashkov, A. S.; Struchkov, Y. T.; Yanovsky, A. I.; Caple, R.; Gybin, A. S.; Anderson, L. G.; Whiteford, J. A. *Tetrahedron Lett.* **1991**, *32*, 2105–2108. (g) Wender, P. A.; de Long, M. A.; Wireko, F. C. *Acta Crystallogr., Sect. C* **1997**, *53*, 954–956. (h) Kuck, D.; Bogge, H. *J. Am. Chem. Soc.* **1986**, *108*, 8107–8109. (i) Bredenkotter, B.; Florke, U.; Kuck, D. *Chem. Eur. J.* **2001**, *7*, 3387–3400. (j) Dullaghan, C. A.; Carpenter, G. B.; Sweigart, D. A.; Kuck, D.; Fusco, C.; Curci, R. *Organometallics* **2000**, *19*, 2233–2236.
- (10) The nomenclature of Keese (ref 7a) has to be modified to specify the location of the nitrogen atom. We propose to designate its location by listing the two rings containing the nitrogen first, then proceeding to the smaller of the remaining two rings. If the two nitrogen-containing rings are of different size, the smaller will be specified first, following Keese.
- (11) (a) Denmark, S. E.; Thorarensen, A.; Middleton, D. S. *J. Am. Chem. Soc.* **1996**, *118*, 8266–8277. (b) Denmark, S. E.; Martinborough, E. A. *J. Am. Chem. Soc.* **1999**, *121*, 3046–3056. (c) Denmark, S. E.; Hurd, A. R. *J. Org. Chem.* **2000**, *65*, 2875–2886. (d) Denmark, S. E.; Herbert, B. *J. Org. Chem.* **2000**, *65*, 2887–2896. (e) Denmark, S. E.; Cottell, J. J. *J. Org. Chem.* **2001**, *66*, 4276–4284.

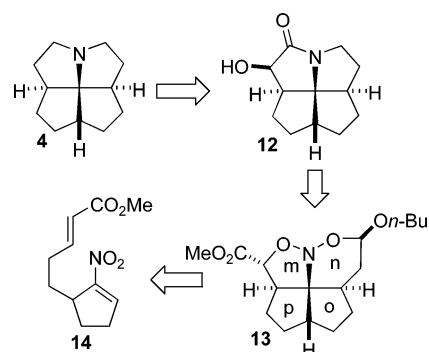
Scheme 2



Results and Discussion

1. *c,c,c,c*-[5.5.5.5]-1-Azafenestrane. 1.1. Retrosynthetic Analysis. Azafenestrane **4** (Scheme 3) should be available from azafenestrane **12** through two-stage deoxygenation (hydroxyl removal and lactam reduction). Lactam **12** is derived from hydrogenolytic unmasking of nitroso acetal **13**, which involves two N–O bond cleavage reactions, a reductive amination, and a lactam formation, all predicted to take place under one set of hydrogenation conditions. Nitroso acetal **13** is the direct product of tandem [4+2]/[3+2] cycloaddition of nitrocyclopentene **14** and *n*-butyl vinyl ether. With regard to the configuration at the ring fusions of nitroso acetal **13** (which in turn will lead to the *c,c,c,c*-1-azafenestrane **3**), only one stereogenic center was expected to be variable. The [3+2] cycloaddition is formally in the spiro mode family¹³ and thus is expected to proceed via an exo-tether mode pathway, which should provide *cis* relationships at the o–p and p–m ring fusions. However, in the [4+2] cycloaddition, the dienophile can approach from either the same face or the opposite face relative to the tethered dipolarophile, which would result in a *trans* or *cis* relationship at the n–o ring fusion, respectively (Scheme 3). Because the least hindered approach should be opposite the tethered dipolarophile, we expected that the favored pathway would lead to a nitroso acetal with configurations at the ring fusions of an *all-cis*-azafenestrane.

Scheme 3

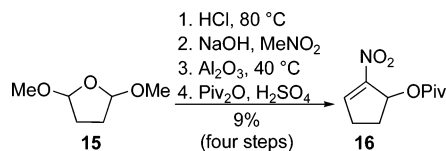


1.2. Synthesis of Nitrocyclopentene 14. The synthesis of nitroalkene **14** required the extension of Seebach's^{14,15} nitroalkylation process to nitrocyclopentenes. Although its nitrocyclohexene analogue was synthesized in good yield,¹⁴ a similar route

- (12) For preliminary communications, see: (a) Denmark, S. E.; Kramps, L. A.; Montgomery, J. I. *Angew. Chem., Int. Ed.* **2002**, *41*, 4122–4125. (b) Denmark, S. E.; Montgomery, J. I. *Angew. Chem., Int. Ed.* **2005**, *44*, 3732–3736.
- (13) Denmark, S. E.; Middleton, D. S. *J. Org. Chem.* **1998**, *63*, 1604–1618.
- (14) Seebach, D.; Calderari, G.; Knochel, P. *Tetrahedron* **1985**, *41*, 4861–4872.
- (15) Knochel, P.; Seebach, D. *Tetrahedron Lett.* **1982**, *23*, 3897–3900.

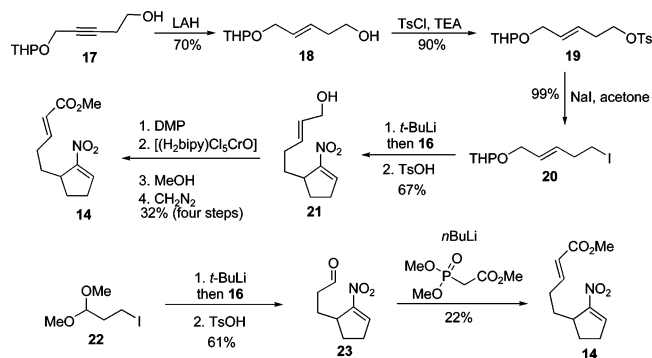
to nitrocyclopentene **16** (Scheme 4) proceeded in only 9% overall yield. Fortunately, all of the materials and reagents needed for the synthesis are readily available and inexpensive.

Scheme 4



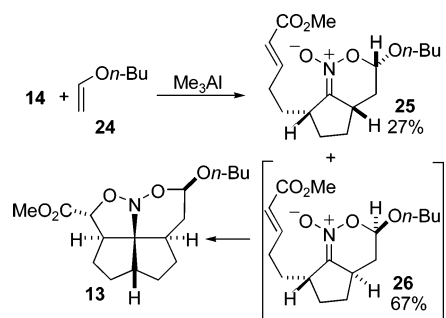
Two different nucleophiles for the nitroallylation were investigated. The first, iodide **20** (Scheme 5), was synthesized from alkyne **17** through adaptation of a literature procedure.¹⁶ Nitroallylation with reagent **16**, followed by deprotection, provided nitrocyclopentene **21** in 67% yield. Unfortunately, two-stage oxidation of **21** and esterification was low yielding (32%), presumably because of the sensitivity of the nitroalkene moiety. A second approach utilized iodide **22**¹⁷ in the nitroallylation to provide aldehyde **23**. It was then necessary to homologate **23** through an olefination reaction, but the overall yield for the synthesis of **14** (~13%) remained unchanged.

Scheme 5



1.3. Tandem Cycloaddition and Completion of the Synthesis. Nitroalkene **14** (Scheme 6) was combined with *n*-butyl vinyl ether (**24**) in the presence of trimethylaluminum, resulting in [4+2] cycloaddition to give two diastereomeric nitronates. The minor isomer **25** results from endo approach of butyl vinyl ether from the same side of the five-membered ring as the tethered α,β -unsaturated ester. The major isomer **26** (endo, opposite side approach) underwent spontaneous spiro-mode¹³ [3+2] cycloaddition, with an exo tether fold, to provide nitroso

Scheme 6



acetal **13** as a single diastereomer with the required configurations at the ring fusions for an *all-cis*-azafenestrane, as confirmed by nuclear Overhauser effect (NOE) NMR experiments (Figure 2).

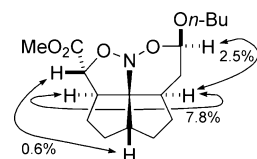
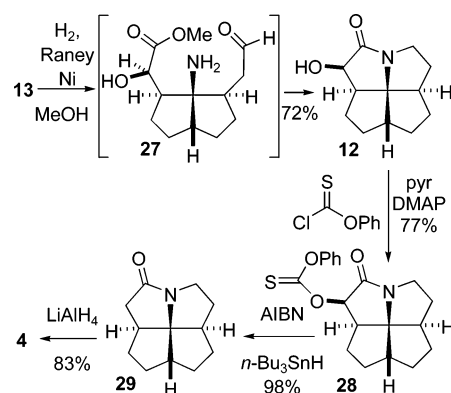


Figure 2. NOE analysis of nitroso acetal **13**.

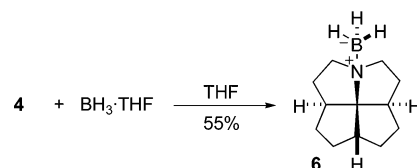
Hydrogenation of nitroso acetal **13** (Scheme 7) in the presence of W-2 Raney nickel in methanol led to N–O bond cleavage, reductive amination, and lactam formation to provide azafenestrane **12** in 72% yield. Therefore, the *all-cis*-azafenestrane ring system was created in only two steps from monocyclic starting material in 48% yield! To complete the synthesis, removal of two oxygen functionalities was required. Thus, alcohol **12** was converted to the corresponding phenyl thionocarbonate **28** in 77% yield and was reduced by a radical-mediated deoxygenation¹⁸ to provide lactam **29** in excellent yield. Finally, reduction of **29** with lithium aluminum hydride provided *c,c,c,c*-[5.5.5.5]-1-azafenestrane **4**.

Scheme 7



1.4. X-ray Crystallographic Analysis of *c,c,c,c*-[5.5.5.5]-1-Azafenestrane·BH₃ (6**).** After treatment of 1-azafenestrane **4** with borane·THF complex (Scheme 8), adduct **6** was obtained as a crystalline solid. Slow evaporation of a saturated solution of **6** in diethyl ether provided colorless needles suitable for X-ray analysis.

Scheme 8



The X-ray crystal structure of **6** (Figure 3) proves its molecular structure and all-*cis* configuration.¹⁹ Although the spectroscopic data for **6** clearly illustrate its symmetry, it crystallizes in a chiral space group resulting from a twist of the four five-membered rings (C(2) is down while C(3) is up, C(5)

(16) (a) Vedejs, E.; Powell, D. W. *J. Am. Chem. Soc.* **1982**, *104*, 2046–2048. (b) Vedejs, E.; Gapinski, D.; Hagen, J. P. *J. Org. Chem.* **1981**, *46*, 5451–5452.

(17) Clive, D. L. J.; Paul, C. C.; Wang, Z. *J. Org. Chem.* **1997**, *62*, 7028–7032.

(18) (a) Barton, D. H. R.; McCombie, S. W. *J. Chem. Soc., Perkin Trans. 1* **1975**, 1574. (b) Barton, D. H. R.; Dorchak, J.; Jaszberenyi, J. C. *Tetrahedron* **1992**, *48*, 7435–7446. (c) Robins, M. J.; Wison, J. S.; Hansske, F. *J. Am. Chem. Soc.* **1983**, *105*, 4059–4065.

is down while C(6) is up, C(8) is down while C(9) is up, and C(11) is down while C(12) is up). Electron diffraction studies on *c,c,c,c*-[5.5.5.5]fenestrane show a similar absence of planes of symmetry.²⁰ The modest planarization at the central carbon (C(13)) is defined by the bond angles N(1)–C(13)–C(7) = 116.1° and C(4)–C(13)–C(10) = 116.6°. Both angles are larger than the 109.5° angle expected for a normal tetrahedral carbon atom. However, these angles are in remarkable agreement with the central angles found for *c,c,c,c*-[5.5.5.5]fenestrane by electron diffraction (116.2°)²⁰ and for the tetrabenzo analogue of *c,c,c,c*-[5.5.5.5]fenestrane (116.5°).^{9h,21} More important than the planarization (which was expected to be low due to the low strain energy of the all-*cis* diastereomer) are the facts that the tandem cycloaddition strategy was validated and that azafenestrane borane complexes can be analyzed crystallographically, which opened the door for the synthesis and X-ray analysis of more strained variants.

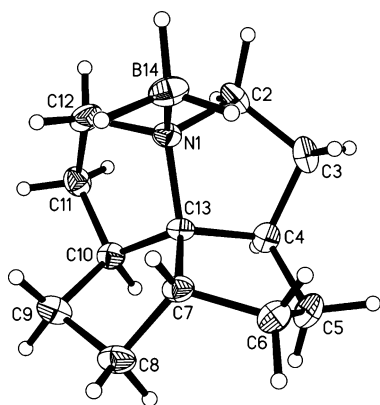


Figure 3. SHELXTL plot of **6** X-ray crystal structure (35% thermal ellipsoids). N(1)–C(13)–C(7) = 116.1°, C(4)–C(13)–C(10) = 116.6°.

2. Synthetic Plan for Strained Azafenestranes. A number of modifications to azafenestrane **4** (Figure 4) could lead to increased planarization of the central carbon atom. These include introduction of a *trans* relationship between rings *n* and *o* (from the minor [4+2] cycloadduct **25**) and reduction in size of one or more of the five-membered rings.

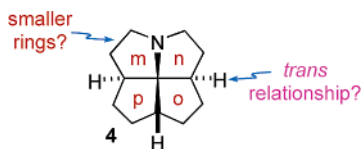
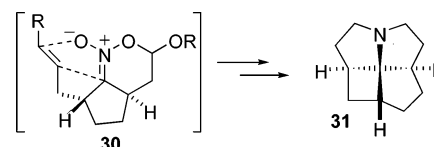


Figure 4. Opportunities for increased planarization.

Of the four rings, ring *n* would be most difficult to contract, because the key hydrogenation step (**13** to **12**) installs a pyrrolidine ring. Ring *o* could be contracted through the use of a nitrocyclobutene as the heterodiene in the [4+2] cycloaddition

step; however, the stability and reactivity of nitrocyclobutenes are unknown, and they are probably prone to polymerization. A four-membered ring *p* could be installed in the azafenestrane ring system through the use of a nitrocyclopentene with a shortened tether to the dipolarophile. To form the four-membered ring, a fused-mode [3+2] cycloaddition would be required (Scheme 9). Although no precedent for fused-mode *nitronate* [3+2] cycloadditions to form four-membered rings exists, one example of a fused-mode intramolecular *nitronate* [3+2] cycloaddition has been reported;²² however, in other cases, nitrones undergo the undesired bridged-mode (reversed regiochemistry) cycloadditions.²³ It is not clear which mode of [3+2] cycloaddition would predominate for a nitronate exocyclic to a five-membered ring, as in **30**.

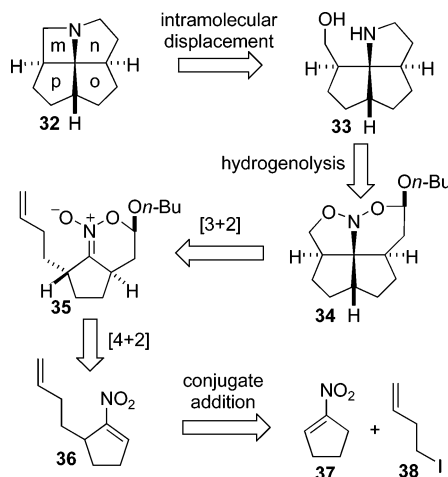
Scheme 9



Of all the rings in the azafenestrane system, replacing ring *m* (**4**, Figure 4) with a four-membered ring could be the simplest plan to obtain increased planarization of the central carbon atom. The details of this modification are presented in the next section.

3. *c,c,c,c*-[4.5.5.5]-1-Azafenestrane. 3.1. Retrosynthetic Analysis. To install an azetidene ring as ring *m* in an azafenestrane, a simplified (as compared to nitroalkene **14**) nitrocyclopentene **36** (Scheme 10) would be required that does not contain an ester moiety on the tethered dipolarophile. We hoped to access 5-(3-butenyl)-1-nitrocyclopentene (**36**) from 1-nitrocyclopentene (**37**) through a conjugate addition reaction, followed by regeneration of the double bond through a selenoxide elimination, rather than building the five-membered ring as in the synthesis of **14**. After [4+2] cycloaddition of nitroalkene **36** with *n*-butyl vinyl ether, which should provide nitronate **35**, an intramolecular [3+2] cycloaddition with an unactivated dipolarophile would be necessary to give nitroso acetal **34**. Simple alkenes have served effectively as dipolarophiles in

Scheme 10



(19) The crystallographic coordinates of **6**, **46**, **52**, **54**, **56**, and **57** have been deposited with the Cambridge Crystallographic Data Centre, deposition nos. CCDC 189803, 262117, 603737, 603736, 262116, and 603735, respectively. These data can be obtained free of charge via www.ccdc.cam.ac.uk/conts/retrieving.html (or from the Cambridge Crystallographic Data Centre, 12 Union Rd., Cambridge CB2 1EZ, UK; fax (+44) 1223-336-033; E-mail deposit@ccdc.cam.ac.uk).

(20) Brunvoll, J.; Guidetti-Grept, R.; Hargittai, I.; Keese, R. *Helv. Chim. Acta* **1993**, *76*, 2838–2846.

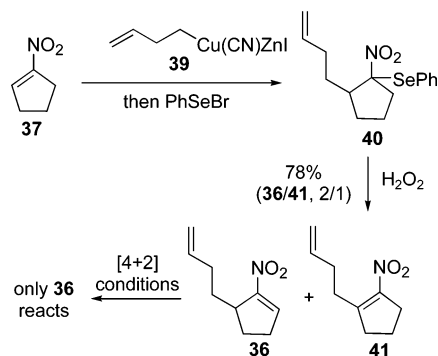
(21) In this context, it is worth mentioning that there is no intrinsic advantage to the study of azafenestranes for discerning the planarization of the central carbon compared to other substituted all-carbon fenestranes. However, the azafenestranes allow a more general approach to various ring sizes and configurations with the option of easy derivatization for crystallinity.

(22) Saito, S.; Ishikawa, T.; Moriwake, T. *J. Org. Chem.* **1994**, *59*, 4375–4377.
(23) (a) Hwu, J. R.; Robl, J. A.; Gilbert, B. A. *J. Am. Chem. Soc.* **1992**, *114*, 3125–3126. (b) Gallos, J. K.; Stathakis, C. I.; Kotoulas, S. S.; Koumbis, A. E. *J. Org. Chem.* **2005**, *70*, 6884–6890.

intramolecular nitronate [3+2] cycloadditions before,²⁴ but not to form *tetracyclic* ring systems. Hydrogenation of nitroso acetal **34** should provide amino alcohol **33**. Then, activation of the alcohol and intramolecular displacement would form azafenes-trane **32**. Simple azetidines have been synthesized from 3-hydroxypropylamines in moderate yields using a modified Mitsunobu reagent.²⁵ Furthermore, the rigidity of the tricyclic amino alcohol **33** should aid in formation of the four-membered ring.

3.2. Synthesis of Nitrocyclopentene 36. A route analogous to that reported for nitroalkene **14** involving nitroallylation¹⁴ was first investigated for the synthesis of **36**. Although the desired target could be obtained, a very poor overall yield (five steps, 8% yield) for the sequence prompted the development of a more efficient synthesis (Scheme 11). Treatment of 1-nitrocyclopentene (**37**)²⁶ with 3-butenylcyanozinc cuprate **39**²⁷ (derived from iodide **38**), followed by trapping of the resulting nitronate²⁸ with phenylselenenyl bromide, provided a mixture of nitro selenide diastereomers **40**. Upon oxidation to the selenoxide, syn elimination gave the desired nitroalkene, **36**, along with its double bond isomer **41** (**36/41**, up to 2/1) in 78% combined yield from 1-nitrocyclopentene. All attempts at chromatographic separation of the two nitroalkenes were unsuccessful. However, the nitroalkene mixture (**36** and **41**) is synthetically useful because the next step of the planned synthesis can effectively separate out the undesired constitutional isomer. In fact, only trisubstituted nitroalkene **36** reacted with *n*-butyl vinyl ether at $-78\text{ }^{\circ}\text{C}$ in the presence of trimethylaluminum (see next section). Therefore, the desired nitroalkene **36** was available in a synthetically useful form in only two steps and 52% overall yield from 1-nitrocyclopentene (**37**), representing a substantial improvement in efficiency over the problematic synthesis of nitroalkene **14**.

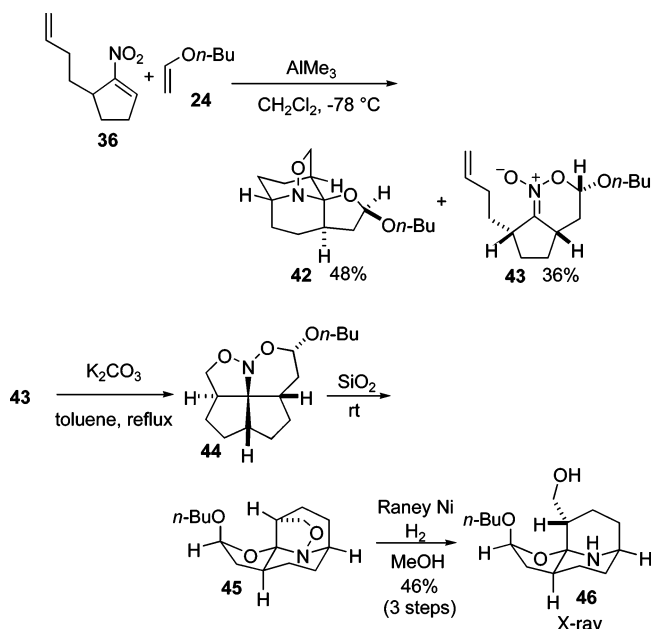
Scheme 11



3.3. Tandem [4+2]/[3+2] Cycloaddition of 36 with 24 and Discovery of a Dyotropic Rearrangement. Treatment of nitroalkene **36** (Scheme 12) with *n*-butyl vinyl ether in the presence of trimethylaluminum at $-78\text{ }^{\circ}\text{C}$ was expected to provide nitroso acetal **34**, the product of tandem [4+2]/[3+2] cycloaddition with approach of the dienophile from the side opposite to the tethered dipolarophile. However, the major product of the reaction was compound **42**, which contained an

azabicyclononane ring system and two five-membered rings! At the time, the identity and origin of this unexpected product were unknown. Nitronate **43** was isolated from the reaction mixture as well, presumably from a [4+2] cycloaddition involving an endo approach of *n*-butyl vinyl ether to the same face that the tethered dipolarophile is disposed, leading to a syn relationship between the two protons at the stereogenic centers in the five-membered ring. Because nitronate **43** was formed, it was reasoned that the expected major product was also formed through tandem cycloaddition, but simply underwent an additional transformation to provide amination **42**. To determine whether a similar process would take place with the minor cycloadduct, a [3+2] cycloaddition was attempted with nitronate **43**. After heating nitronate **43** in toluene in the presence of potassium carbonate, analysis of the reaction mixture confirmed the formation of nitroso acetal **44**. However, upon purification by silica gel column chromatography, a new product, **45**, was formed that was clearly a diastereomer of the major product of the initial tandem cycloaddition attempt, **42**.

Scheme 12



The structure of amination **45**, and, by analogy, of its diastereomer **42**, was confirmed by X-ray crystallographic analysis of hydrogenation product **46**, in which the only N–O bond has been cleaved (Figure 5).¹⁹

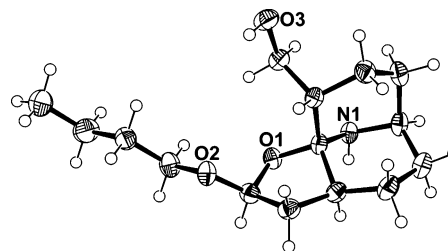


Figure 5. ORTEP X-ray crystal structure of **46** (30% thermal ellipsoids).

A hypothesis on the origin of the unexpected amination **42** and **45** became clear upon analysis of a molecular model of nitroso acetal **44** (Scheme 13). Because the nitroso acetal **44** and amination **45** share the same molecular formula, the conversion of **44** to **45** requires a simple molecular reorganization. The rearrange-

(24) Denmark, S. E.; Senanayake, C. B. W. *Tetrahedron* **1996**, *52*, 11579–11600.

(25) Sammes, P. G.; Smith, S. J. *Chem. Soc., Chem. Commun.* **1983**, 682–684.

(26) Corey, E. J.; Estreicher, H. *J. Am. Chem. Soc.* **1978**, *100*, 6294.

(27) Knochel, P.; Yeh, M. C. P.; Berk, S. C.; Talbert, J. *J. Org. Chem.* **1988**, *53*, 2390–2392.

(28) Denmark, S. E.; Marcin, L. R. *J. Org. Chem.* **1993**, *58*, 3850–3856.

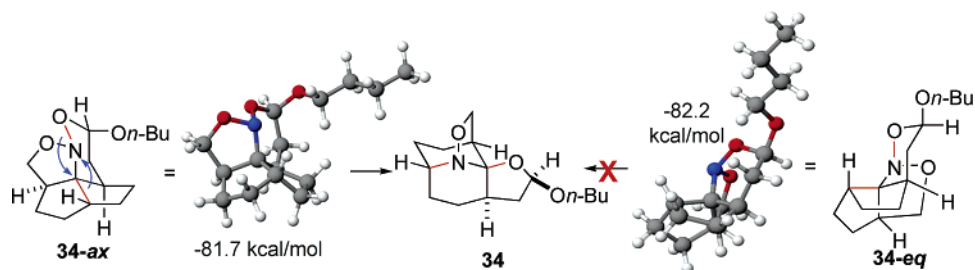
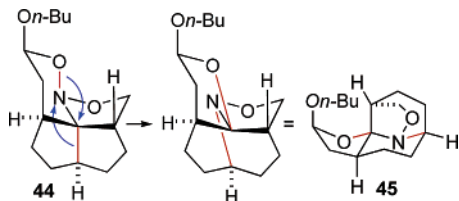


Figure 6. Nitroso acetal **34** conformers and PM3 minimized energy structures with heats of formation.

ment involves breaking both an N–O bond and a C–C bond and forming a C–O bond and a C–N bond. Analysis of a 3D representation of nitroso acetal **44** clearly shows the two breaking bonds (red) in near-perfect antiperiplanar alignment. The ensuing transposition, where two σ bonds exchange position, is known as a dyotropic rearrangement.²⁹ Presumably, this reaction is driven to completion via the increased thermodynamic stability of the aminal product **45**. The exact role of silica gel in promoting the rearrangement remains obscure, but hydrogen bonds or proton transfer from Si–OH moieties may trigger the process.

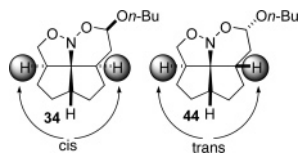
Scheme 13



3.4. Conformations of Nitroso Acetal 34. Through conformational analysis of nitroso acetal **34** (Figure 6), the expected major product of the tandem cycloaddition reaction, a means to prevent the rearrangement became apparent.³⁰ Two different chair conformers of the six-membered ring in nitroso acetal **34** are possible. In the first, **34-ax**, the 1,2-oxazine ring adopts a conformation that places the butyloxy group in an (anomericly stabilized) axial orientation. This conformation exhibits the required stereoelectronic alignment of the two migrating bonds (red); thus, the rearrangement takes place readily to give aminal **42**. However, in a second low-energy conformation, depicted in structure **34-eq**, a chair-flip has occurred and the breaking bonds (red) are no longer in alignment. By favoring this conformer, the rearrangement should be suppressed, and hydrogenolysis should provide the desired tricyclic amino alcohol **33**. Minimization (PM3 level) of the two conformers of nitroso acetal **44**, beginning from perfect chair geometry, resulted in local minima that were within 0.5 kcal/mol in energy of one another. The minimized energy structures have distorted chair forms, but both conformers retain the axial/aligned and equatorial/not aligned relationship present in the perfect chair analogues.

(29) Reetz, M. T. *Adv. Organomet. Chem.* **1977**, *16*, 33.

(30) The nitroso acetals **34** and **44** are derived from the different facial approaches of the dienophile to the nitrocyclopentene and give different stereochemical relationships of the ring fusion hydrogens.

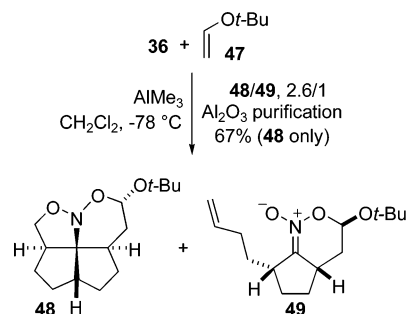


On the basis of these calculations, it was hypothesized that destabilizing the axial conformer or stabilizing the equatorial conformer should increase the barrier to rearrangement. The use of larger vinyl ethers should destabilize the axial conformer through steric interactions. Alternatively, a change in selectivity in the [4+2] cycloaddition from endo to exo would provide a nitroso acetal epimeric at the anomeric center. In this manifold, the misaligned conformer would benefit from anomeric stabilization, which could also suppress the rearrangement. A bulkier vinyl ether might also bring about this change in selectivity; therefore, it was decided to try *tert*-butyl vinyl ether in the [4+2] cycloaddition.

3.5. Suppression of the Rearrangement and Completion of the Synthesis.

In the event, tandem cycloaddition of *tert*-butyl vinyl ether (**47**) with nitroalkene **36**, promoted by Me₃Al at –78 °C (Scheme 14), led to formation of nitroso acetal **48** (exo selectivity!) with no rearrangement under the reaction conditions, thus providing support for the proposed hypothesis. Analysis of the crude reaction mixture revealed a 2.6/1 ratio of nitroso acetal **48** (exo dienophile approach from the opposite side as the tethered dipolarophile) to the minor nitronate **49** (exo dienophile approach from the same side as the dipolarophile), which did not undergo spontaneous [3+2] cycloaddition. Purification of the crude reaction mixture by silica gel chromatography did lead to partial dyotropic rearrangement of nitroso acetal **48**; however, chromatography with basic alumina allowed for isolation of a 67% yield of **48** without rearrangement.

Scheme 14



The stereochemical assignment of nitroso acetal **48** (formed by exo-selective addition) was carried out through ¹H NMR NOE analysis (Figure 7). The reversal in selectivity in the [4+2] cycloaddition must be derived from increased steric interactions in the endo transition state (**50**, Figure 8) between *tert*-butyl vinyl ether and the trimethylaluminum complexed to the nitroalkene. Relief of these steric interactions is available with an exo approach (**51**), and this transition state leads to the experimentally observed nitroso acetal **48**. Although further studies are needed to determine the generality of this method,

the reversal of selectivity could be synthetically useful as an alternative to bulky aluminum Lewis acids in cases where *exo* selectivity is desired.

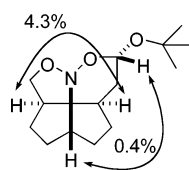


Figure 7. Observed NOEs for nitroso acetal **48**.

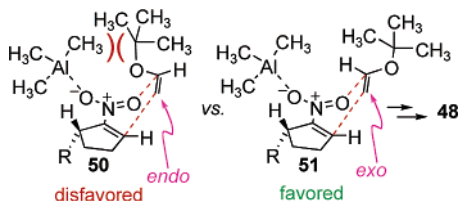
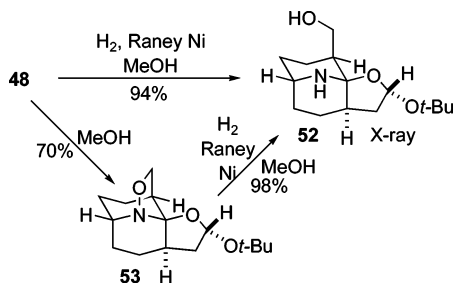


Figure 8. [4+2] *endo* and *exo* transition states and outcomes.

With nitroso acetal **48** in hand, we were poised to complete the synthesis in short order. Unfortunately, standard hydrogenolysis conditions (H_2 , Raney Ni, MeOH) provided the reduced, rearranged product **52** (Scheme 15) in 94% yield, with no sign of the desired azafenestrane precursor **33**. An X-ray crystal structure of aminal **52** confirmed its structure and configuration and provided further support for the reversal in selectivity noted in the [4+2] cycloaddition (acetal configuration corresponds to *exo* selectivity).¹⁹ An investigation of reaction conditions (solvents, acidic additives, basic additives) uncovered the fact that protic solvents induced the dyotropic rearrangement. In fact, simply stirring nitroso acetal **48** in methanol at room temperature provided aminal **53** in 70% yield after purification. This aminal **53** could also be reduced to amino alcohol **52** in 98% yield using standard hydrogenation conditions, suggesting its intermediacy in the conversion of nitroso acetal **48** to amino alcohol **52**.

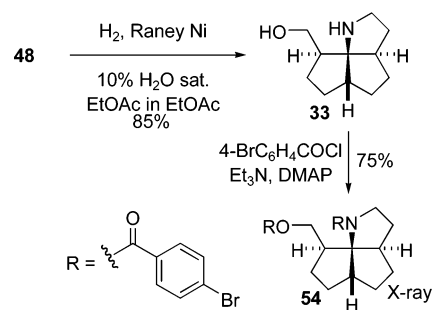
Scheme 15



Because rearrangement of **48** took place upon hydrogenolysis, new conditions had to be developed that would allow for reduction of nitroso acetal **48** to the desired amino alcohol **33** (Scheme 16) before the dyotropic rearrangement could take place. Attempts to carry out the hydrogenation in non-protic, dry solvents (EtOAc, THF) were unsuccessful; however, rearrangement did not take place under these conditions either. In the end, it was discovered that, by adding a controlled amount of water to the reaction in the form of water-saturated ethyl acetate (10% in dry ethyl acetate, 0.25 M), the desired hydrogenolysis took place to give amino alcohol **33** in 85% yield while still suppressing the rearrangement. In fact, under these conditions, no formation of aminal **52** was observed at

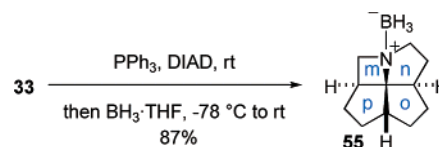
all. The structure and stereochemical assignment of amino alcohol **33** (corresponding to a “broken” *all-cis*-azafenestrane) were verified through X-ray crystallographic analysis of its bis-4-bromobenzoyl derivative **54**, which was formed in 75% yield from **33**.¹⁹

Scheme 16



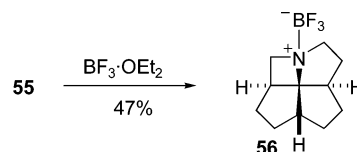
At the outset of the synthesis, a major challenge was thought to be the formation of the strained azetidine ring. However, treatment of amino alcohol **33** (Scheme 17) under standard Mitsunobu^{25,31} coupling conditions (triphenylphosphine, diisopropylazodicarboxylate (DIAD), 1.0 equiv each) led to formation of the desired azafenestrane, which was efficiently isolated (i.e., separated from triphenylphosphine oxide and DIAD- H_2 byproducts) as its borane complex *c,c,c,c*-[4.5.5.5]-1-azafenestrane· BH_3 (**53**) in 87% yield. Thus, despite all of the setbacks along the way, **55** is available from 5-butenyl-1-nitrocyclopentene **36** in only three steps and 50% overall yield, demonstrating the power of the tandem nitroalkene cycloaddition reaction for rapidly building molecular complexity.

Scheme 17



3.6. X-ray Crystallographic Analysis of *c,c,c,c*-[4.5.5.5]-1-Azafenestrane· BF_3 (56**).** To quantify the planarizing distortions at the central carbon atom in **55**, an X-ray structure was required. Although the azafenestrane borane adduct is a crystalline solid, crystals suitable for X-ray diffraction could not be obtained. Adduct **55** was soluble in many organic solvents, and thin needles could be obtained from hexane at low temperature, but multiple attempts to collect X-ray diffraction data were unsuccessful. Fortunately, simple treatment of **55** with boron trifluoride etherate promoted exchange to the crystalline BF_3 adduct **56** (Scheme 18). Cooling of a warm, saturated solution of **56** in hexane to room temperature deposited X-ray-quality crystals.¹⁹

Scheme 18



(31) Mitsunobu, O. *Synthesis* **1981**, 1–28.

The BF_3 adduct of *c,c,c,c*-[4.5.5.5]-1-azafenestrane (**56**) crystallized in a centrosymmetric, unambiguous space group. Molecule **56** has three unique conformations occupying the same site (forms 1, 2, and 3, Figure 9). Oddly, both enantiomers exist in different proportions at this site. Inversion of symmetry generates the enantiomer of each conformation at a separate site within the unit cell.

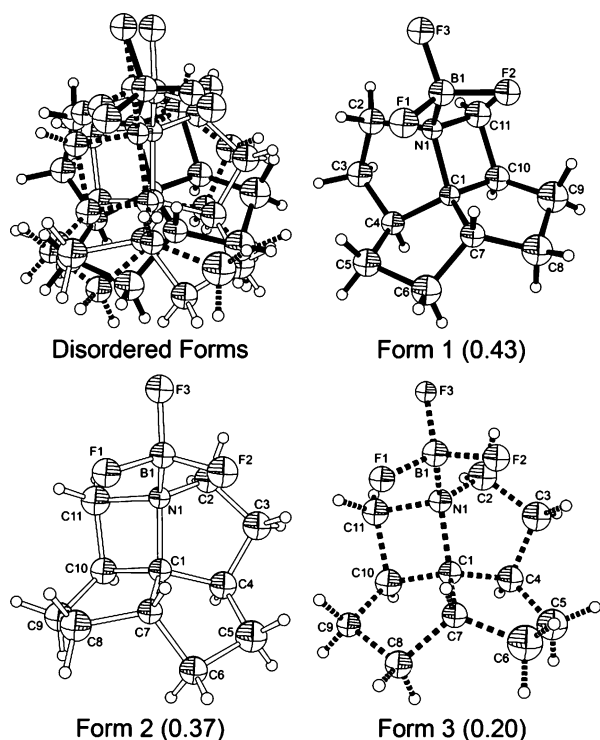


Figure 9. Labeled SHELXTL plots of **56** depicting forms 1, 2, and 3 (relative site occupancy) with displacement spheres drawn at 35% probability for non-H atoms.

The assignment of atomic sites belonging to each form was carried out via bond length correspondence. No other assignment maintains a reasonable correlation between chemically equivalent C–C and C–N bonds. Of particular interest in fenestrane chemistry are the two distorted angles around the central tetrasubstituted carbon (Table 1). All of the forms have similar angles around C(1), with average values for angles N(1)–C(1)–C(7) and C(4)–C(1)–C(10) of 120.3(10)° and 121.3(11)°, respectively. None of the C(1) angles differ by more than 1 su from the mean.

Table 1. Central Angles (deg) for **56**

	C(4)–C(1)–C(10)	N(1)–C(1)–C(7)
form 1	120.7(8)	119.8(7)
form 2	121.2(10)	119.2(8)
form 3	121.9(13)	121.8(12)

Azafenestrane **56** was primarily synthesized to quantify the deviation of the central carbon from typical tetrahedral geometry. In this case, crystal packing forces failed to isolate a unique geometry, so the question of which form best represents the low-energy conformation of the compound remained unclear. The relative geometries of the three forms of **56** are depicted as best-fit overlays in Figure 10. From this representation, it is clear that the three forms differ mainly in the conformations of

the five-membered rings A, B, and C. These equilibrations are clearly enumerated by changes in dihedral angles terminating at bridgehead atoms N(1), C(4), C(7), and C(10). Converting form 1 to form 2 requires opposing flips of rings A and C; torsion N(1)–C(2)–C(3)–C(4) rotates 69(2)° and C(7)–C(8)–C(9)–C(10) rotates –63(2)°. Converting form 1 to form 3 requires flips of rings A and B; N(1)–C(2)–C(3)–C(4) rotates 69(3)° and C(4)–C(5)–C(6)–C(7) rotates 52(3)°. And, converting form 2 to form 3 requires ring B and C flips; C(4)–C(5)–C(6)–C(7) rotates –52(3)° and C(7)–C(8)–C(9)–C(10) rotates –67(3)°.

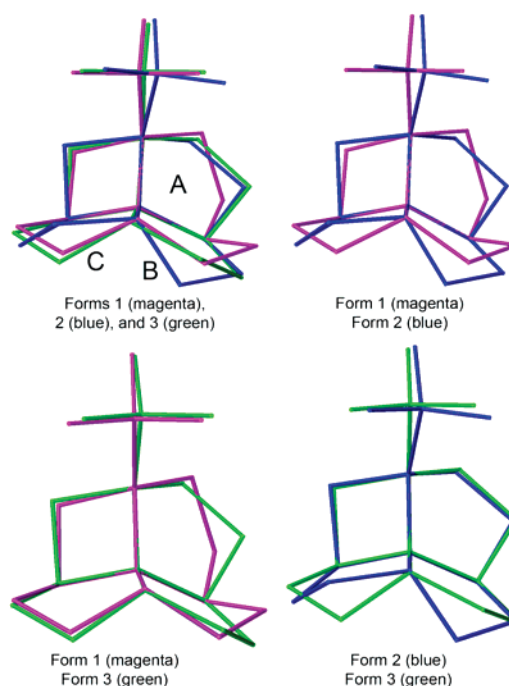


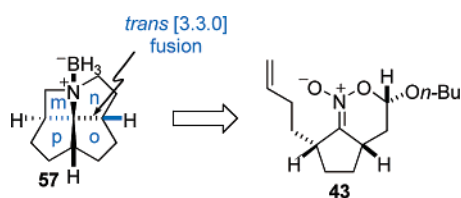
Figure 10. Best-fit overlays of the same enantiomer of the three forms of **56** viewed roughly down the C(7)–C(1) bond.

Relative site occupancies suggest form 1 is most stable within this crystal environment. Calculations reveal very little energy difference between forms 1 and 2 but a slight increase for form 3. With respect to form 1, the relative ΔH_f for forms 2 and 3 are respectively –0.15 and +3.69 kcal/mol (AM1) and +0.65 and +3.79 kcal/mol (PM5). The relative total energies for forms 2 and 3 are respectively +0.09 and +4.39 kcal/mol (DFT B88-LYP). These energy differences are small with respect to crystal packing forces. Because the two most populated forms are enantiomeric, the unit cell is most likely composed of a static distribution of locally ordered forms. The lattice can readily accommodate either enantiomer of **56** in form 1, 2, or 3 as the crystal grows. If azafenestrane **56** had been synthesized enantioselectively, it is likely that less disorder would be present in the solid state.

4. *t,c,c,c*-[4.5.5.5]-1-Azafenestrane·BH₃. 4.1. Retrosynthetic Analysis. Because the [4+2] cycloaddition of nitroalkene **36** and *n*-butyl vinyl ether (**24**) leads to two different diastereomeric nitronates (the major nitronate undergoes [3+2] cycloaddition and dyotropic rearrangement, but the minor nitronate **43** is isolated; see section 3.3), opportunity for the synthesis of an even more strained azafenestrane with a trans relationship at the n–o ring fusion existed (Scheme 19). Therefore, investiga-

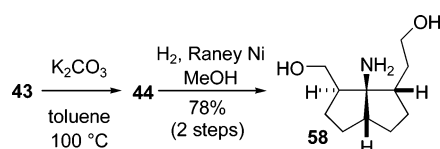
tions on the conversion of nitronate **43** into *c,t,c,c*-[4.5.5.5]-1-azafenestrane·BH₃ (**57**) were pursued.

Scheme 19



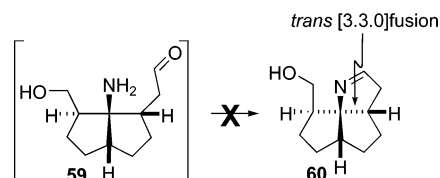
4.2. Forward Synthesis. Intramolecular [3+2] cycloaddition of nitronate **43** (Scheme 20) was promoted by heating it in the presence of potassium carbonate to provide nitroso acetal **44** that contains a trans-fused [4.3.0] ring system. As described earlier, nitroso acetal **44** underwent dyotropic rearrangement when purified on silica gel. However, if **44** was subjected to the standard hydrogenation conditions (H₂, Raney Ni, MeOH) without purification, the rearrangement could be suppressed. Unfortunately, the expected reductive amination to form a pyrrolidine ring did not take place. Instead, the amino diol **58** was isolated from the reaction mixture in 78% yield from nitronate **43**.

Scheme 20



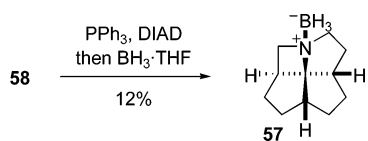
Presumably, during the reduction, the expected aldehyde intermediate **59** (Scheme 21) failed to undergo intramolecular imine formation (which is normally followed by imine reduction to complete the reductive amination). In hindsight, this failure is not surprising, because imine **60** contains a highly strained trans-fused [3.3.0] bicyclic system. Because the reductive amination does not take place, the aldehyde was simply reduced under the reaction conditions to the corresponding alcohol **58**. Clearly, a different reaction is needed to build systems with so much strain.

Scheme 21



Because the reductive amination did not proceed, a double Mitsunobu reaction was investigated to complete the synthesis (Scheme 22). Treatment of amino diol **58** with 3.0 equiv each of triphenylphosphine and DIAD led to formation of the desired azafenestrane, which was again isolated as its borane adduct

Scheme 22



57, albeit in only 12% yield. As might be expected, undesired intermolecular processes compete with the desired reaction pathway.

4.3. X-ray Crystallographic Analysis of *c,t,c,c*-[4.5.5.5]-1-Azafenestrane·BH₃ (57**).** Fortunately, adduct **57** was a highly crystalline material, and cooling of a saturated solution of **57** in pentane provided crystals suitable for X-ray crystallographic analysis (Figure 11).¹⁹ As expected, the introduction of a trans fusion in the azafenestrane skeleton results in significant planarization of the central carbon atom. The angle N(1)–C(1)–C(7) is 126.3°, corresponding to a 16.8° deviation from normal tetrahedral geometry. The increased strain of the molecule is also apparent by simple visual inspection of the geometry around C(4). The flattening of the most distorted bond angle (C(3)–C(4)–C(5) = 129.4°) is also brought about by the trans fusion within the azafenestrane skeleton.

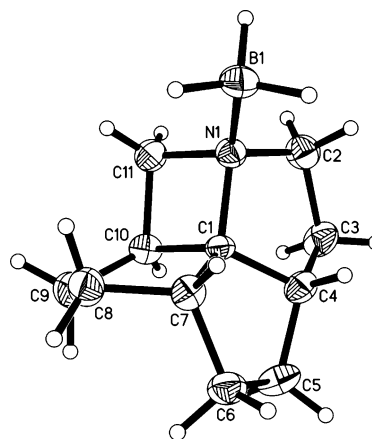


Figure 11. SHELXTL plot of X-ray crystal structure of azafenestrane **57** (35% thermal ellipsoids). N(1)–C(1)–C(7) = 126.3°, C(4)–C(1)–C(10) = 120.7°.

5. Density Functional Theory (DFT) Calculations on 1-Azafenestrans. **5.1. Relative Strain Energy.** Two diastereomeric 1-azafenestrans (*c,c,c,c*- and *c,t,c,c*-) from various families ([5.5.5.5], [4.5.5.5], [4.5.5.4], [4.5.4.5], [4.5.4.4], and [4.4.4.4]) were subjected to a CONFLEX³² search (a systematic search for low-energy conformers at the MM3 level) to provide a number of local minimized energy structures (Figure 12). Each local minimum was then further minimized at PM3 and then DFT B88-LYP levels, and the total energy of the lowest energy structure for each compound was tabulated. Direct comparison of total energies for molecules with the same number and types of atoms provides relative strain energy. However, as ring sizes decrease, CH₂ groups are removed, and their contribution to the total energy must be taken into account. Fortunately, a method for the required adjustment has been reported.³³ Minimization of straight-chain hydrocarbons (propane, butane, pentane) using the same basis set and determination of the energy contribution for an unstrained CH₂ group were performed. Subtracting this value for each four-membered ring in 1-azafenestrans provides a convenient method to obtain relative strain energies for similar compounds with different molecular formulas. Normalization of all the energies to that of *c,c,c,c*-[5.5.5.5]-1-azafenestrane **4** (0.0 kcal/mol) results in the relative strain energies depicted in Figure 12.

(32) CAChe WorkSystem Pro Version 6.1.12.33; Fujitsu Ltd.: 2004.

(33) Dudev, T.; Lim, C. *J. Am. Chem. Soc.* **1998**, *120*, 4450–4458.

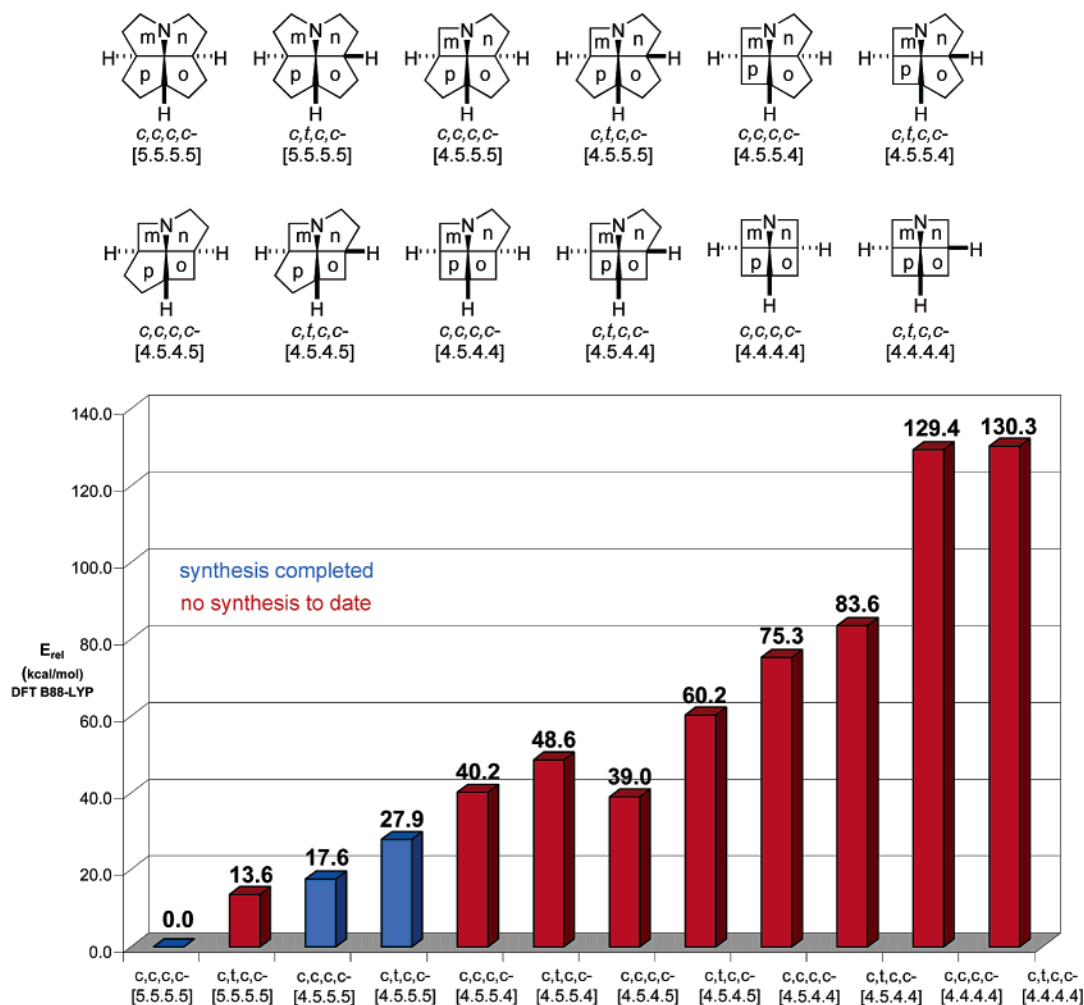


Figure 12. Relative strain energies (DFT B88-LYP) of select 1-azafenestranes.

c,t,c,c -[4.5.5.5]-1-Azafenestrane, the free form of the most strained azafenestrane synthesized to date (57), has a calculated strain energy 27.9 kcal/mol higher than that of c,c,c,c -[5.5.5.5]-1-azafenestrane 4, the first synthetic azafenestrane. The question often arises of what the limit is in strain energy for isolability of azafenestranes. This is a very difficult question to answer because strain is distributed throughout the entire molecule. In a highly simplistic analysis, one can estimate a limit based on a carbon–carbon bond strength of 83–85 kcal/mol³⁴ to be around the strain energy of c,t,c,c -[4.5.4.4]-1-azafenestrane, and in fact, a substituted fenestrane with this skeleton has yet to be synthesized. The most strained fenestrane reported is a c,c,c,c -[4.4.4.5]fenestrane,^{9d} and its central angles were determined to be 128° and 129°. Because a carbon–nitrogen bond (69–75 kcal/mol³⁴) is weaker than a carbon–carbon bond, this reasoning suggests that the limit for azafenestranes is the incorporation of two four-membered rings (strain energy less than 69 kcal/mol). However, the fallacy of this argument is easily shown by the strain energy of cubane (162 kcal/mol), which is much greater than the bond dissociation energy of a carbon–carbon single bond, and yet cubane is isolable and stable.³⁵

5.2. Central Angle Calculations. A graph of the central angles for the global minimum energy structures used in the previous section for strain energy calculations is presented in Figure 13. As predicted, as ring sizes decrease and trans relationships are introduced, central angle values increase (increased planarizing distortion). The more strained of the two central angles tracks with the stereochemical relationships; that is, in the *all-cis*-azafenestranes, the C–C–C central angle (magenta squares data series) is larger, while in the c,t,c,c -1-azafenestranes, the N–C–C angle (blue diamonds data series) has more distortion. The calculated angles are in good agreement with those observed for azafenestrane borane adducts from X-ray crystallographic analysis (largest deviation is 2.4° for the C–C–C angle in c,t,c,c -[4.5.5.5]-1-azafenestrane), suggesting that borane complexation to the nitrogen atom in azafenestranes does not lead to significant changes in structure. Finally, with a few exceptions, the average value of the two azafenestrane central angles (red triangles data series) steadily increases as more and more strained azafenestranes are analyzed.

Conclusion

The use of the tandem [4+2]/[3+2] cycloaddition of nitroalkenes for the synthesis of strained 1-azafenestranes has been documented, and a method for derivatization and X-ray analysis of 1-azafenestranes through their borane (or BF₃) adducts has

(34) Smith, M. B.; March, J. *March's Advanced Organic Chemistry: Reactions, Mechanisms, and Structure*, 5th ed.; John Wiley & Sons: New York, 2001.

(35) Roux, M. V.; Dávalos, J. D.; Jiménez, P.; Notario, R.; Castaño, O.; Chicks, J. S.; Hanshaw, W.; Zhao, H.; Rath, N.; Liebman, J. F.; Farivar, B. S.; Bashir-Hashemi, A. *J. Org. Chem.* **2005**, *70*, 5461–5470.

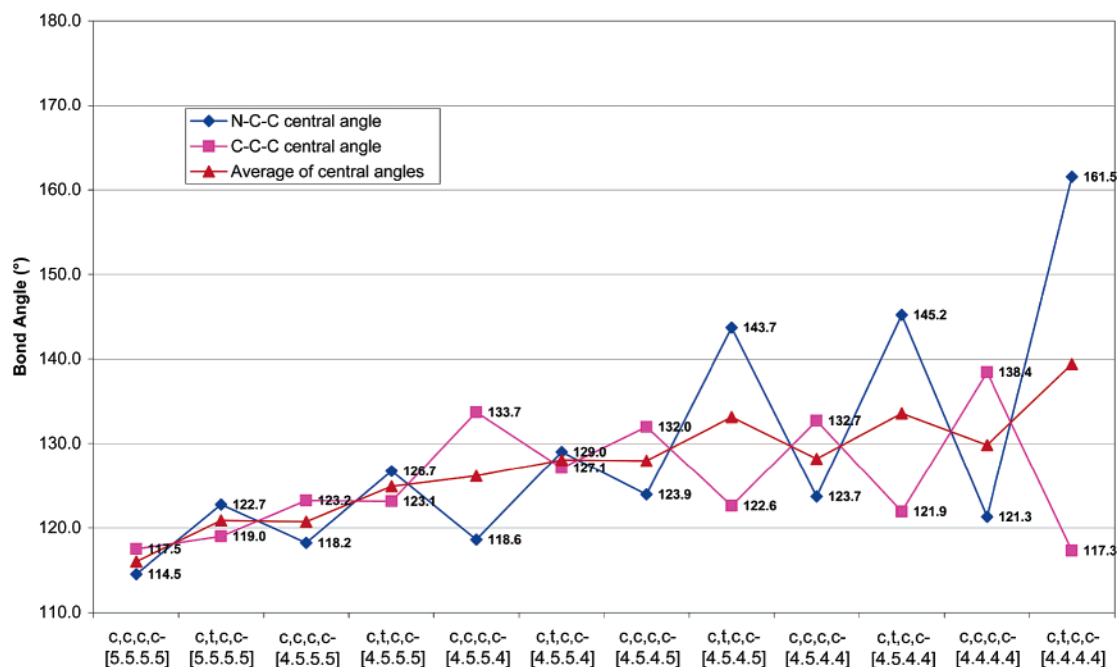


Figure 13. Calculated central angles for global minimum energy structures (DFT B88-LYP) of select 1-azafenestranses.

been developed. The synthesis of the relatively unstrained *c,c,c,c*-[5.5.5.5]-1-azafenestrane **4** was accomplished in 29% yield from nitrocyclopentene **14**, and its borane adduct displayed modest planarization of the central carbon atom (central angles of 116.1° and 116.6°).

In addition, the efficient (five steps and 26% overall yield) synthesis of the more strained *c,c,c,c*-[4.5.5.5]-1-azafenestrane·BH₃ **55** was completed. Although **55** could not be analyzed crystallographically, its boron trifluoride adduct **56** was amenable to X-ray analysis, and increased planarization was observed (average central angles of 120.3° and 121.3°).

Moreover, an azafenestrane bearing a trans-fused bicyclo-[3.3.0]octane unit was also available from a minor product from the key cycloaddition reaction. The X-ray crystal structure of its borane adduct, *c,t,c,c*-[4.5.5.5]-1-azafenestrane·BH₃ **57**, displayed deviation from tetrahedral geometry of 16.8° for the N–C–C central angle, and **57** is the most strained azafenestrane synthesized to date.

During the course of the synthesis of the [5.5.5.4]-1-azafenestranses, an unexpected dyotropic rearrangement was discovered that converts nitroso acetals into tetracyclic amins. The rearrangement seems to be controlled by the conformation of the six-membered ring in the nitroso acetal precursors. By utilizing a bulky vinyl ether and developing new hydrogenation conditions, the rearrangement was suppressed, allowing for the completion of the synthesis of the desired azafenestranses.

Finally, theoretical calculations on the azafenestranses were carried out at the DFT B88-LYP level in order to estimate relative strain energy and predict central angles. The free form of the most strained synthetic azafenestrane **57** has 27.9 kcal/mol more strain energy than the first synthetic azafenestrane **4**. Furthermore, calculated central angles are in good agreement with those observed in X-ray crystal structures of azafenestrane borane derivatives. Efforts toward even more strained azafenestranses as well as investigations on dyotropic rearrangements of nitroso acetals are in progress and will be reported in due course.

Acknowledgment. We are grateful to the National Institutes of Health (GM30938) for generous financial support. J.I.M. thanks the Procter & Gamble Co., Abbott Laboratories, and Johnson & Johnson for graduate fellowships. We thank Scott R. Wilson and Teresa Prussak-Wieckowska of the UIUC George L. Clark X-Ray Facility for collection and interpretation of X-ray data.

Supporting Information Available: Full characterization of all products, detailed experimental procedures, details on calculations, and crystallographic information files, in CIF format. This material is available free of charge via the Internet at <http://pubs.acs.org>.

JA0632759